A Model Study of Aggregation of Acetylene Molecules

Kimberly Shuler and Clifford E. Dykstra*

Department of Chemistry, Indiana University−Purdue University Indianapolis, 402 North Blackford Street, Indianapolis, Indiana 46202

Received: August 8, 2000; In Final Form: October 16, 2000

An interaction potential previously developed for the acetylene dimer was applied to small and large clusters of acetylene molecules. With the inclusion of the effects of vibrational dynamics via quantum Monte Carlo techniques, the calculation of rotational constants of the trimer and tetramer gave a very good assessment for the use of the interaction potential with more than two interacting molecules. Calculations performed on larger clusters reveal trends in the energetics of aggregation and in the preferred arrangement of acetylenes. The pentamer is found to have essentially the structure of the cyclic tetramer with the additional molecule above and in the center of the ring. By continuing to very large clusters of up to 391 interacting molecules, it is clear in what ways the features of the crystal structures of acetylene appear in small clusters. Estimates of the lattice energy were accomplished through a limited extrapolation of the cluster results. The static-structure interaction energies of the cubic and orthorhombic crystals were found to be quite close, but with the high-temperature form being the lower by about 12% of the interaction energy. A number of refinements were evaluated to provide understanding of the delicate balancing of competing effects that are responsible for the existence of the two crystal forms of solid acetylene.

Introduction

From a detailed picture of the bonding in the acetylene dimer, clusters of larger sizes can be investigated to gain insight into the manifestations of the acetylene−acetylene interaction in aggregation and perhaps in the structure and energetics of acetylene in the solid phase. The equilibrium structure of the acetylene dimer has been studied experimentally and is known to have a T-shaped geometry.[1−11] It can interconvert to an equivalent form with the monomers' roles interchanged by passing through a slipped parallel structure of C_{2h} symmetry. Ab initio studies[12−19] not only have confirmed this finding but also have provided a basis for constructing intermolecular potential surfaces suitable for dynamical analysis. In our recent study,[19] a potential surface was developed from ab initio calculations using four parameters and electrical properties intrinsic to the monomers. The four parameters were empirically adjusted so that the rotational constants of the vibrational ground state matched spectroscopically determined values to 0.1%. Because of the form of the interaction potential, it can be directly applied to any number of interacting acetylenes, and with the objective of understanding key features of acetylene aggregation, we report results of such calculations here.

The acetylene trimer and tetramer are the two larger acetylene clusters whose structures have been established spectroscopically.[20,21] Both ab initio calculations[22−28] and modeling studies[27,29] have been successful in showing the cyclic form of these clusters. The T-shaped arrangement preferred in the dimer can be regarded as persisting in these cyclic structures, though with considerable distortion in the trimer. There is insufficient data from the experimental study of the pentamer[20] for a full characterization; however, ab initio studies of this cluster provide certain insight into the possible equilibrium structure.[22−24]

Although it is difficult to study the physical properties of solid acetylene due to its explosive nature, the structure of two solid phases have been determined by X-ray and neutron powder diffraction studies.[30−37] Both phases exhibit hydrogen bonding features in that there are T-shaped pairs of monomers in each. At a temperature of 133 K, there is a first-order phase transition between the high-temperature cubic phase with *Pa*3 symmetry and the orthorhombic phase with *Acam* symmetry. This phase transition requires a rotation of the acetylenes that lie parallel to the body diagonals of the cubic unit cell from their out-of-plane arrangement to a new equilibrium position which is planar. Both theoretical[38,39] and experimental[40−44] studies of the solid-state polymerization of acetylene have shown that a cross-linked product results from applying pressure to the low-temperature or high-pressure phase with orthorhombic symmetry.

The existing body of information provides a limited connection between the gas-phase clusters and the solid. The cluster information extends at most to five interacting monomers, and the modeling and molecular dynamics efforts[45−55] basically start at the condensed phase. With our model of the acetylene−acetylene interaction, which includes certain cooperative effects as discussed below, we have sought to provide a picture of aggregation beyond the pentamer and to determine how structural features in the crystalline forms of acetylene relate to the structures in small and medium-sized clusters.

Theoretical Approach

Equilibrium structures and stabilities of various $(HCCH)_n$ clusters were calculated with a form of the interaction potential incorporated into the molecular mechanics for clusters (MMC) scheme[56] for intermolecular interaction potentials. The MMC potential is a sum of the classically evaluated electrical interaction energy plus an atom−atom Lennard-Jones or 6−12 nonelectrical potential with parameters designated *c* and *d*. MMC *c* and *d* parameters are assigned to sites, usually atomic centers, in a molecule, and the complete potential, *V*, for a

* Author to whom correspondence should be addressed.

10.1021/jp002872t CCC: $19.00
Published on Web 11/17/2000

collection of molecules is

$$V = E_{\text{electrical}} + \sum_{A>B}^{\{\text{molecules}\}} \sum_{i}^{\{\text{sites on A}\}} \sum_{j}^{\{\text{sites on B}\}} \left(\frac{d_i d_j}{r_{ij}^{12}} - \frac{c_i c_j}{r_{ij}^{6}} \right) \quad (1)$$

The electrical representation employed to evaluate $E_{\text{electrical}}$ for clusters of acetylene molecules consists of the molecule-centered quadrupole moment, and the dipole and quadrupole polarizabilities, all of which have been obtained via extensive ab initio calculations.[57] Our prior work on the acetylene dimer[19] included examination of other electrical representations, each with selected *c* and *d* parameters. The representation used here, designated CQ-ACCD for central quadrupole and based on coupled cluster level potential surface points, showed the best overall suitability. With the sites for the 6−12 terms in eq 1 being the hydrogen and carbon atoms, there are only four unique parameters needed for calculations on any $(HCCH)_n$ cluster. These four parameters from the CQ representation[19] were selected on the basis of having the MMC potential match interaction energies obtained from large basis, correlated ab initio calculations, and then were refined with a series of vibrational ground-state calculations so as to match spectroscopic rotational constants. The *c* and *d* parameters are 6.4 and 3560 au for carbon and 0.8 and 11.43 au for hydrogen, respectively.

The effect of mutual or back polarization versus direct polarization can be compared within the MMC scheme. It is not surprising in view of acetylene's zero-valued dipole moment that polarization is a small effect, and hence, back polarization is very small. In tests we carried out, back polarization had around a 3% effect on the interaction energy for clusters of up to 10 acetylenes. As well, there is an effect of back polarization on structural parameters, though this is also small. For instance, in the tetramer, back polarization changes the distances between monomers by about 0.2%. The effect of back polarization on the primary rotational constants of clusters of 3, 4, 6, and 8 acetylenes is up to a 1% increase. Given the small size of this contributor to the interaction, it was neglected for most subsequent calculations, and except where specifically indicated otherwise, all values reported here were obtained without including mutual polarization in the potential. Doing this means that the potential has up to 3-body interactions (via direct polarization). We note that the MMC parameters were selected[19] in calculations on the dimer that only included direct polarization.

The process of searching for equilibrium structures of $(HCCH)_n$ clusters ($n < 20$), especially the larger of these, involved repeated searches with different initial geometries. Certain of these initial geometries were selected to maximize the number of pairs of acetylenes arranged in a T-shaped form. Other initial geometries were selected by adding one or two acetylenes at a long separation distance from some optimized smaller structure. And still other initial geometries were selected by deleting monomers one at a time from the optimized structure of a larger cluster until all combinations had been tested. Force constant evaluations were used to ensure that minima were always located. Numerous local minima were found. The determination that global minima were found is to the extent that with our wide variety of starting configurations, especially those based on similarly sized clusters, no further lowering of a cluster's energy was obtained. In addition, special searches were performed on certain clusters whose initial symmetry corresponded to the cluster being a fragment of the orthorhombic or cubic crystalline forms. This was usually done two ways, maintaining the symmetry as a constraint, or fully relaxing the structural parameters.

MMC calculations were performed on several $(HCCH)_n$ clusters whose size ($n > 20$) makes them more representative of crystal fragments than are clusters of just a few acetylenes. Calculations on crystal fragments were performed to optimize the unit cell parameters as well as the angular orientation of the individual molecules for both the cubic and orthorhombic phases. The only constraint placed on the equilibrium searches for these clusters was to maintain the symmetry as either orthorhombic or cubic. A full optimization of structural parameters (i.e., without constraints or imposed symmetry) was also performed for a crystal fragment with 79 monomers.

Using the CQ representation for the MMC model potential, vibrational analysis was performed for clusters of acetylene up to $(HCCH)_{13}$ via rigid body diffusion quantum Monte Carlo (RBDQMC) calculation.[58−61] Since the higher frequency intramolecular vibrational motions are excluded due to monomer rigidity, longer time steps can be used for a given precision in the simulation. For the RBDQMC calculations reported here, the time step was 4.0 au [1.0 au (time) or 1.0 $h/(2\pi E_h)$ = 2.41888×10^{-17} s]. The number of QMC-psips was 10 000, and the energy and property evaluations were performed through 180 000 time steps each. These were carried out following an equilibration sequence that consisted of at least 20 000 time steps of decreasing size and an overall duration of 6×10^5 au. Rotational constants were calculated by continuous averaging of the inverses of the principal moments of inertia. More direct connection with spectroscopic measurement is obtainable from calculations that yield rotational excited-state energies and sets of transition energies such that rotational constants can be obtained following the same analysis applied to spectroscopic data.[62,63] We expect the error from the averaging approach to be small and comparable to other lingering error sources, such as the assumed rigidity of acetylene.

Results and Discussion

Structures of Small Acetylene Clusters. The MMC equilibrium structures of the two smallest acetylene clusters studied are shown in Figure 1. The acetylene trimer consists of a planar cyclic structure wherein each pair of monomers takes on a distorted T-shaped arrangement. A T-shaped configuration maximizes the attractiveness of the quadrupole−quadrupole interaction among monomers, a relatively strong element for the acetylene−acetylene interaction. In the tetramer, this arrangement among pairs is accomplished with less distortion than in the trimer, though the monomers are twisted somewhat out of plane. A comparison of MMC structural values for the trimer and tetramer with ab initio results is presented in Table 1.

The structure of the tetramer has an interesting S_4 symmetry. Notice that if two lines were drawn connecting mass centers of opposed (not adjacent) pairs of acetylenes, they would be nonintersecting lines because the four mass centers are not coplanar (Figure 1), a result that has been found from ab initio calculations on the tetramer.[23] The optimum planar form, though, is little different in its energy because in both planar and nonplanar forms, every pair of acetylenes has an orientation that is essentially 90°, the T-shape that is optimum for the quadrupole−quadrupole interaction. Hence, an important energetic feature we find is that the cluster can invert through a planar transition state with a very small barrier, which the MMC potential gives as 23 cm^{-1}.

In Table 2, a comparison of rotational constants determined from RBDQMC with spectroscopic values for the dimer, trimer,

TABLE 1: Calculated Equilibrium Structural Parameters[a] and Rotational Constants for $(HCCH)_3$ and $(HCCH)_4$

	R_1 (Å)	R_2 (Å)	θ_1 (deg)	θ_2 (deg)	$A_{eq} = B_{eq}$ (MHz)	C_{eq} (MHz)
$(HCCH)_3$ MMC (this work)	2.473		39		1941	970
ab initio (Bone et al.[26])	2.478		42		1931	965
ab initio (Brenner et al.[25])	2.460		42			
$(HCCH)_4$ MMC (this work)	2.789	0.823	39	27	997	586
ab initio, planar constrained[b] (Bone et al.[23])	3.007		45		1011	506

[a] The structural parameters for the trimer are R_1, the distance between the C_3 symmetry axis and a monomer's mass center, and θ_1, the angle between the molecular axis of a monomer and the line from its mass center to the C_3 axis. The tetramer is a nonplanar cyclic structure with its monomer centers alternatively R_2 above and below the plane that contains the cluster's center of mass and is perpendicular to the S_4 symmetry axis. R_1 is the distance from a monomer's mass center to the S_4 symmetry axis. Each acetylene is twisted by an angle designated θ_1 about an axis passing through its center of mass and parallel to the S_4 axis. θ_2 is an elevation angle relative to the plane that includes a monomer's mass center and is perpendicular to the S_4 axis. [b] For comparison with the ab initio calculation, the MMC potential yields $R_1 = 3.028$ Å with a planar constraint.

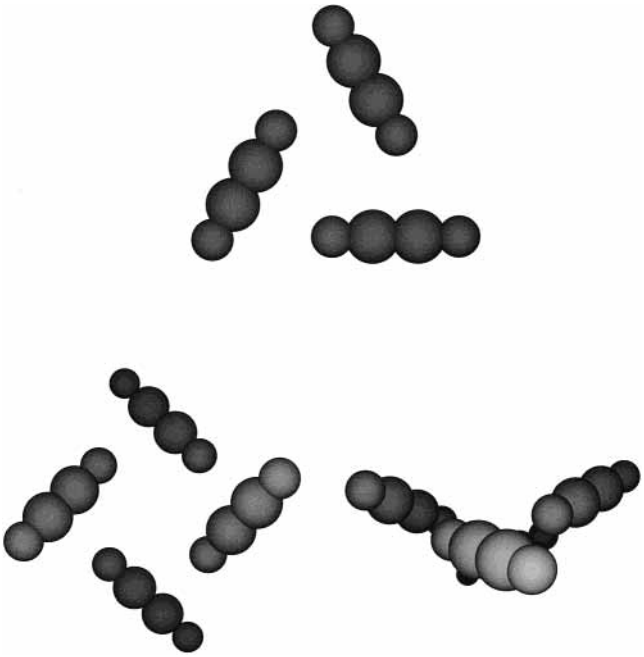

Figure 1. Equilibrium structures of the acetylene trimer and tetramer obtained from MMC calculations. Both clusters are cyclic. The second view of the tetramer is with the S_4 axis is in the plane of the page.

TABLE 2: Vibrational Ground-State Rotational Constants of Small Acetylene Clusters

	rotational constant[a] (MHz)			calculated difference[a] from equilibrium value (percent)
	calculated			
cluster	equil.	vib. g.s.[c]	expt.[c]	
$(HCCH)_2$	1901	1856 [19]	1856.6 [3]	−2.4
$(HCCH)_3$	1941	1882	1885.8 [21]	−3.0
$(HCCH)_4$	997	973	972.5[b] [20]	−2.5
$(HCCH)_6$	522	505		−3.3
$(HCCH)_8$	310	301		−3.0
$(HCCH)_{10}$	202	195		−5.8
$(HCCH)_{12}$	151	140		−7.3
$(HCCH)_{13}$	132	127		−3.8
$(DCCD)_2$	1725	1689 [19]	1688.2 [7]	−2.1
$(DCCD)_3$	1759	1711		−2.7
$(DCCD)_4$	909	889		−2.2
$(DCCD)_6$	478	463		−3.1

[a] Values are $\langle A + B \rangle/2$ except for the dimer, for whcich the value is $\langle B + C \rangle/2$. [b] Reported as $B'' = 0.03244$ cm^{-1}. [c] Reference numbers are included in brackets.

and tetramer is presented. Mostly, the calculated values are very close to the experimentally determined values for the three clusters in both proton and deuterated forms. For the tetramer, the calculated value is within 1 MHz of the spectroscopic value for B[20] and about 16 MHz for C ($C_{MMC} = 578$ and $C_{expt} = 594.5$ MHz[20]), the largest difference from experiment that was found. The agreement is an indication that the MMC potential developed for the acetylene dimer provides a good representation for clusters of several acetylene, making it meaningful to use the model potential to examine certain features of aggregation. We note that the electrical part of the MMC potential includes 3-body or cooperative interaction terms via the electrical polarization energetics.

Using the MMC potential, a search for the global minimum of larger acetylene clusters was performed. As one way of selecting favorable initial arrangements of the monomers in larger clusters, we tried to maximize the number of T-shaped pairings, i.e., the number of occurrences of a T-shaped or near T-shaped orientation between neighboring acetylenes. The first step was finding the structure of the pentamer. Since the trimer is planar while the tetramer is not, a number of both planar and nonplanar initial geometries were selected for the pentamer in order to search for its global minimum. It was found that the equilibrium structure for the pentamer had a nonplanar arrangement of acetylenes in which one molecule lies above what is essentially a tetramer arrangement of the other four molecules (Figure 2), a "4 + 1" structure. An ab initio study at the SCF level with a polarized double-ζ basis[23] restricted to two "probable lowest-energy conformations" gave as the lowest energy pentamer structure a planar, double-ring butterfly form with C_{2h} symmetry. A planar cyclic form of C_{5h} symmetry was slightly higher in energy.[23] Another ab initio study at a lower level of treatment[22] predicted that the optimum cyclic structure is nonplanar. The double ring structure was found to be a local minimum on our MMC potential surface; however, the ease of geometry optimization with the model potential allowed us to examine the surface extensively and to locate a different structure as the global minimum. In terms of the number of favorable quadrupole−quadrupole interactions, the cyclic C_{5h} structure has 5, the double-ring C_{2h} structure has 6,[23] and the "4 + 1" structure (Figure 2) that we find to be the global minimum has 8. The 8 T-shaped pairings in the pentamer are illustrated in Figure 2.

The equilibrium structure of the hexamer was found to resemble the tetramer and pentamer in having a four-membered ring, with the extra two monomers above and below the plane of this core tetramer as shown in Figure 3. These two monomers are able to arrange to have more than one favorable T-shaped pairing with the molecules in the ring and thereby form another tetramer-like structure within the hexamer. In this way, the six-membered cluster achieves a quasi-cubic symmetry with the six acetylene molecules nearly equivalent to one another and the number of T-pairings being 12. To be more specific, this cluster retains the S_4 symmetry of the tetramer, meaning that there are four equivalent acetylenes in a ring. The acetylenes above and below are a chemically equivalent pair and are twisted 90° relative to each other when viewed along an axis that runs

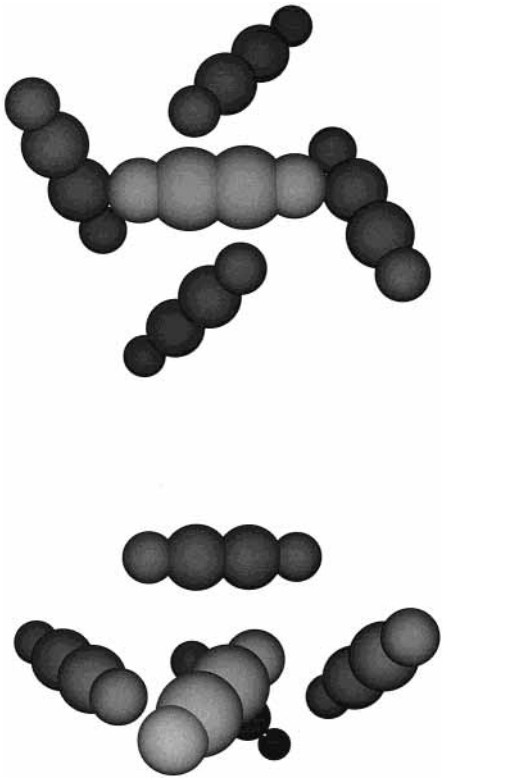

Figure 2. Equilibrium structure of the acetylene pentamer obtained from MMC calculations. The top view is looking down the C_2 symmetry axis, while the bottom view, from the side, shows there is one molecule above the plane of a tetramer-like ring. The top view shows how the acetylene above the ring accomplishes near T-shaped arrangements with the molecules in the ring.

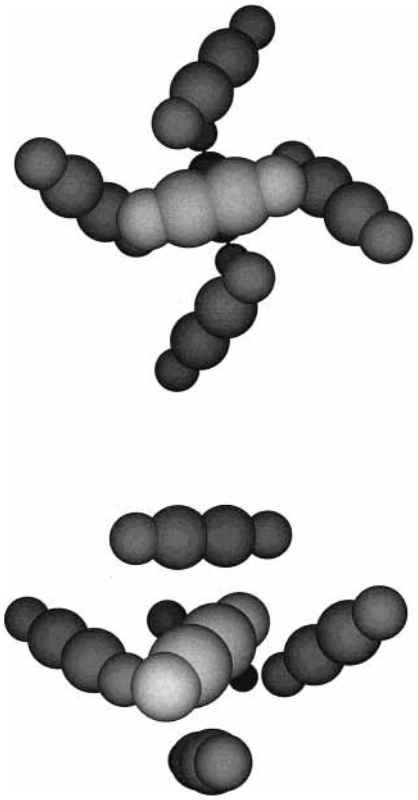

Figure 3. Equilibrium structures of the acetylene hexamer obtained from MMC calculations. The S_4 symmetry axis is perpendicular to the plane of the page in the top view and parallel in the bottom.

through their mass centers. A small distortion can shift the S_4 rotation axis to either of the other two axes; in other words, there exists a series of interconversion pathways among equivalent conformations.

The 13-membered cluster has a quite regular equilibrium structure, as shown in Figure 4, and it has a total of 36 T-shaped pairings. The 10- and 12-membered clusters resemble the 13-membered cluster somewhat, but with missing members. On the other hand, this is not seen with a cluster of eight acetylenes where the molecules distort from the regular positions and orientations they would have in the 13-membered cluster in order to fill the spaces of the otherwise regular arrangement.

Vibration and Energetics. RBDQMC rotational constants for clusters with up to 13 acetylenes are given in Table 2 along with the percentage difference for each value from the corresponding value associated with the equilibrium structure. Vibrational averaging diminishes the sizes of the rotational constants as vibrational excursions along the anharmonic potential make the clusters effectively larger. Deuterium substitution of the acetylene clusters yields the normal isotope effect of diminishing equilibrium and vibrationally averaged rotational constants and by slightly diminishing the sizes of the vibrational averaging effects. Clusters with 10 and 12 acetylenes show relatively greater vibrational averaging effects on the rotational constants, consistent with these two being incomplete forms of the regular 13-membered cluster. The incompleteness allows for greater vibrational excursions or greater floppiness.

Results given in Table 3 show an increasing stiffness with respect to weak vibrational modes as cluster size increases. Zero-point energies (ZPE) of the clusters expressed on a per monomer basis increase from 121 cm^{-1} in the trimer to around 190 cm^{-1} in the hexamer and the next few clusters. At 13, there is another step in the zero-point energy per monomer to 234 cm^{-1}. This is consistent with the 13-membered cluster being an essentially closed structure (Figure 4). The per monomer ZPE is likely to continue to increase with increasing cluster size as the relative number of molecules that are interior versus surface grows. As discussed below, our calculations indicate 340 cm^{-1} as the limiting value for the per monomer ZPE in large clusters.

Table 4 gives the MMC stabilities of the equilibrium structures of the clusters of up to 19 monomers and of a 79-membered cluster. For the smaller clusters, the change in the interaction energy from adding another acetylene molecule is given to show that there are energetically preferred numbers of molecules, e.g., 13. Again, this corresponds to completing or nearly completing fairly regular arrays versus having open positions or dangling molecules. Another comparison of the energetics is obtained by considering how many pairings of monomers exist, that is, how many times two monomers are found to be at distances comparable to the acetylene−acetylene separation distance in the dimer (i.e., at separations $\leq$4.5 Å). This number has been calculated from the optimized structures and is given in Table 4 as the value *M*. Cluster interaction energy divided by the cluster's value of *M* changes more uniformly than does the incremental energy difference from adding a monomer. This points to the fact that the pairwise interactions are the most significant and that essentially all close approaches (pairings) of monomers in the clusters manage to take on the favorable T-shaped arrangement or be close to that.

From the values in Table 4 for the largest clusters, a value of 360 cm^{-1} seems to be roughly the energetic contribution for an interacting pair of monomers in a large cluster of acetylenes. This is also seen by a calculation of the energy of a 201-molecule cluster, though with a fixed, not optimized, cubic-like structure. This structure has 940 pairings, and the energy on a per pairing basis is 352 cm^{-1}. Notice that this is about

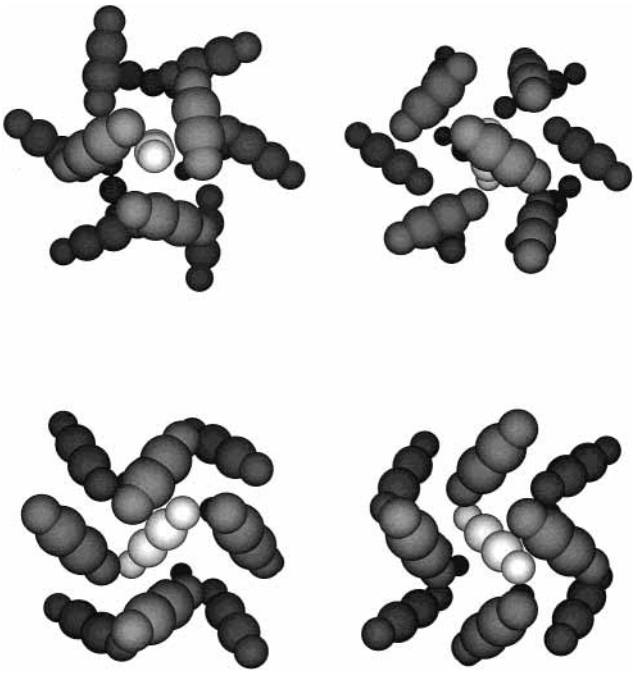

Figure 4. Calculated equilibrium structure of $(HCCH)_{13}$. The central molecule has been shaded much more lightly to distinguish its position in each of the different views shown. In the upper left, the central molecule is perpendicular to the plane of the page and it is surrounded by 12 monomers arranged in three layers. These layers consist of a distorted trimer in the front, a six-membered pinwheel in the middle, and another distorted trimer in the back. Each trimer layer contributes 3 distorted T-shaped pairings. In addition, each monomer in the trimer layer also forms a distorted T-shaped pairing with two monomers from the middle ring as well as one with the central molecule giving 18 T-shaped pairings. The six-membered pinwheel layer contributes 6 distorted T-shaped pairings from the ring and 6 from T-shaped pairing of each member of the ring with the central molecule. Another view (upper right) is that obtained by rotating the cluster $-45°$ about the *a* axis, the horizontal axis in the plane of the page through the center of the cluster. Applying a second rotation, this one by 45° about the *b* axis, the vertical axis in the plane of the page through the center of the cluster, yields the third view (bottom left) showing the cubic features of the cluster. Finally, a further 90° rotation about the *a* axis yields the cluster (bottom right) with the *c* axis in the plane of the page.

TABLE 3: Ground Vibrational State Zero-Point Energies of Acetylene Clusters from MMC/RBDQMC Calculations

number of monomers, N	zero-point energy, ZPE (cm^{-1})	ZPE/N (cm^{-1})
2	131	66
3	362	121
4	533	133
5	750	150
6	1135	189
8	1507	188
10	1907	191
12	2304	192
13	3036	234

70% of the correspondingly calculated value for the dimer. Within our model potential, this diminishment can arise from long-range unfavorable interactions, three-body polarization effects, and the inability to form a large aggregation with every pairing being a perfect T-shaped arrangement. The last of these appears as the main source of diminishment, and consequently, one recognizes an energetic compromise in having numerous pairings that are near, not perfect, T-shaped arrangements rather than having fewer pairings that are more perfectly T-shaped.

As cluster size increases, monomer separations can be diminished via an increasing effect of cooperative (many-body) interactions as included here via polarization energetics and via pairwise interactions with next nearest neighbors. Values in the last column of Table 4 illustrate the contraction obtained in our calculations for acetylene clusters. These values are the smallest separations between the mass centers of any two monomers in the clusters. The minimum separation distance is about 0.2 Å less in the 79-monomer cluster than in the dimer.

TABLE 4: MMC Equilibrium Stabilities of Acetylene Clusters

number of monomers, N	number of T-pairings, M	incremental stability $D_e(N) - D_e(N-1)$ (cm^{-1})	stability per pair, D_e/M (cm^{-1})	smallest separation distance (Å)
2	1	503	503	4.333
3	3	1010	504	4.283
4	4	847	590	4.274
5	8	936	412	4.174
6	12	1117	368	4.162
7	11	983	491	4.175
8	14	1200	471	4.163
9	18	1161	431	4.178
10	21	1242	429	4.176
11	25	1218	409	4.109
12	29	1429	402	4.116
13	36	1721	371	4.189
14	38	1196	383	4.134
15	43	1276	368	4.131
16	47	1229	363	4.122
17	52	1291	353	4.131
18	54	1384	366	4.143
19	60	1368	352	4.148
79	333		358	4.109

Crystal Fragments. We next applied our interaction model to both solid phases of acetylene, orthorhombic (*Acam*) (Figure 5) and cubic (*Pa*3) (Figure 6). Structures with finite numbers of molecules were constructed by surrounding a central molecule with acetylenes in successive shells, maintaining the symmetry of the given crystalline form. The "core" consisted of 17 acetylenes and the distance cutoffs that corresponded to adding one molecular thickness at a time-produced larger clusters of 79, 201, and 391 acetylenes. Within the symmetry constraints of either a cubic or orthorhomic crystal, structural parameters were optimized. Table 5 gives the optimized unit cell parameters obtained from these calculations. It can be seen that there is good convergence of these parameters with increasing cluster size.

To assess the extent to which the presence of surface molecules affected the unit cell parameters, further calculations on the 79-, 201-, and 391-membered crystal fragments were performed wherein unit cell parameters of each layer or shell of the crystal were optimized individually. The core cluster of 17 molecules at the center of the crystal has no surface acetylenes and its structure should be least affected by the presence of surface acetylenes on the outer shells. Results from this series of calculations showed that the original unit cell parameters, from the uniform optimization of the crystal fragments, were very close to the average of the unit cell parameters when each shell's structure was optimized individually. More important, the differences among the unit cell parameters from individual optimization for each shell were so small as to affect the density based on the core's structural parameters by less than 0.6%. In other words, the limited optimization of the crystal fragments was sufficient and surface effects were not significant in the cores of the largest clusters.

The optimum form of the cluster of 13 monomers resembles the cubic crystal (Figure 4), not the orthorhombic structure, and that is clearly the preferred aggregation pattern at the level of small clusters. With fewer than 13 monomers, there are quite

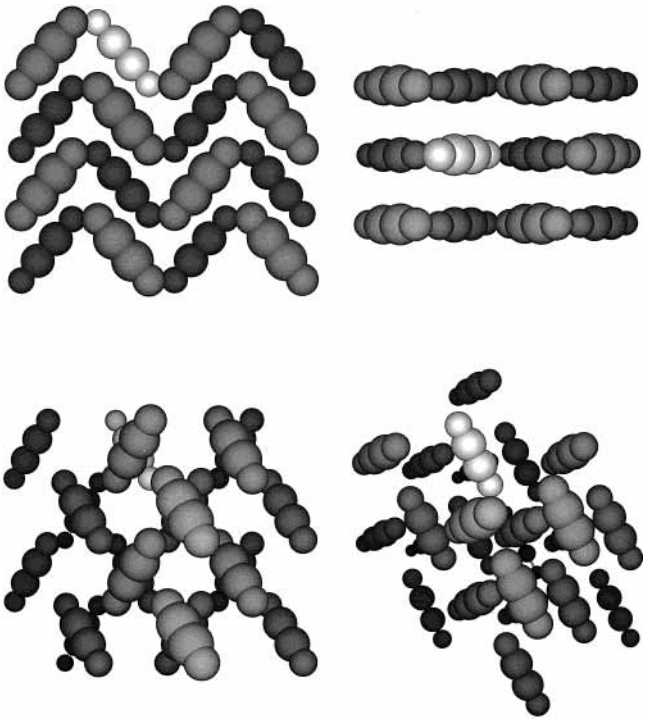

Figure 5. Structure of the orthorhombic crystal of acetylene. In each view, one molecule has been shaded much more lightly in order to help with visualization. In the top left structure, a lighter shading identifies the acetylenes that occupy a plane which is *c*/2 above those that are have the darker shading. The top right structure is achieved by rotating the top left structure by 90° about the *a* axis which lies horizontally in the plane of the page through the center of the cluster. In this view, the three layers, each separated by *c*/2, illustrate the planarity of the orthorhombic crystal. This third plane cannot be seen in the top left structure because it is directly beneath the plane that contains the lighter-colored acetylenes. Following from the top left to the lower left, the cluster has been rotated by 45° about the *b* axis which lies vertically in the plane of the page through the center of the cluster. Rotating the cluster about the *a* axis which lies horizontally in the plane of the page through the center of the cluster by 45° brings us to the lower right structure, where the T-shaped arrangement of acetylenes is most evident.

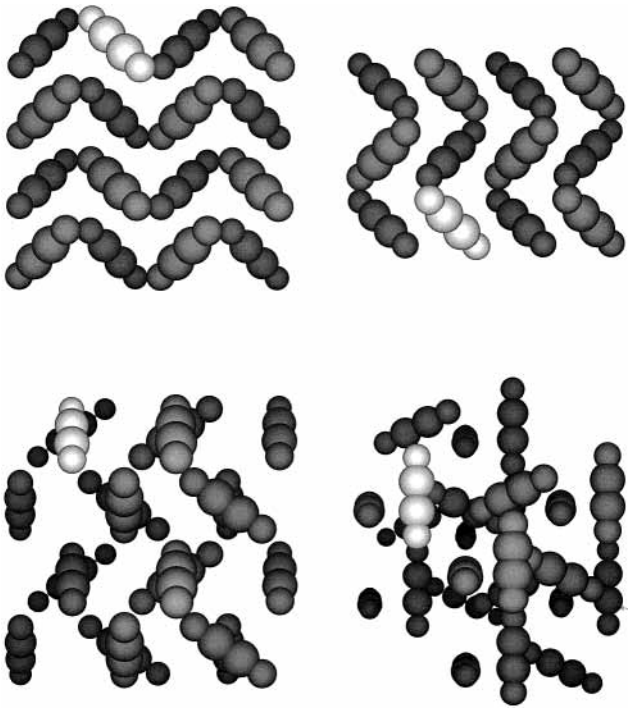

Figure 6. Structure of cubic crystal of acetylene. In each view, the same molecule has been shaded differently in order to help with visualization. The ordering of the structures in this figure follows the same pattern of rotations as the orthorhombic crystal in Figure 5.

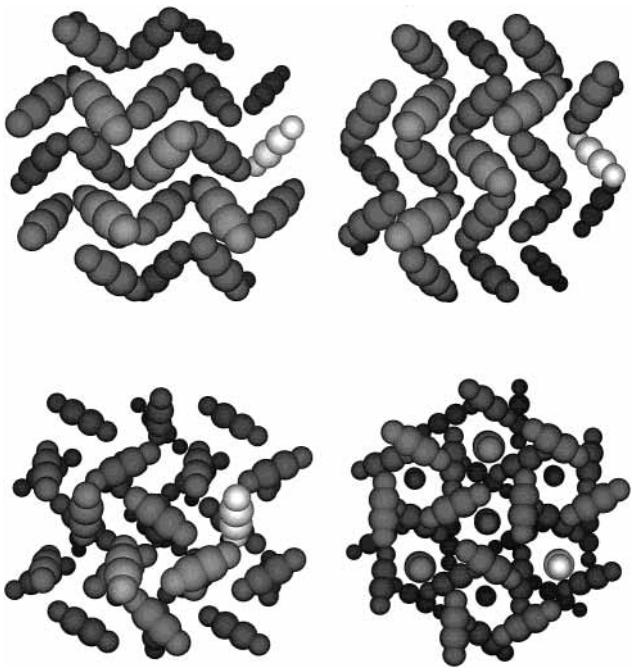

Figure 7. Calculated equilibrium structure of $(HCCH)_{37}$. In each view, the same molecule has been shaded differently in order to help with visualization. The ordering of the structures in this figure follows the same pattern of rotations as the orthorhombic crystal in Figure 5.

noticeable differences from the cubic crystal form, but certain of these differences turn out to involve distortions with small energy effects. For instance, in the hexamer, the monomers above and below the four-membered ring have a perpendicular orientation, yet where this grouping is identified within the cubic crystal, these two monomers are parallel. We carried out MMC calculations to re-optimize the structure of the hexamer under the constraint that these two monomers are parallel. The destabilization due to imposing this constraint turns out to be small, 23 cm^{-1}, and that this structure is a local minimum on the potential surface. So, while at first glance the hexamer may not reveal itself as being like the cubic crystalline form, in fact, the difference follows from its potential surface being shallow for twisting these two molecules oppositely. Hence, with increasing size, the small clusters fairly quickly take on structural characteristics of the infinite crystal, and importantly, of the cubic not orthorhombic form. The energetic reason for this difference is that there are 6 T-pairings per monomer in the cubic form and only 4 pairings in the orthorhombic form (Figures 5 and 6). Furthermore, the pairings in the orthorhombic form are half T-shaped and half "slipped parallel," a form which is about 80 cm^{-1} less stable in the dimer.[19] That is, a monomer in the cubic form has a near T-shaped pairing with 12 nearby molecules, but a monomer in the orthorhombic form has only 8 nearby molecules and it is T-shaped with 4 and slipped parallel with the other 4.

Comparing the 391-membered crystal fragment results to experimental unit cell parameters (Table 5), we find that the model results for the cubic phase are around 1% smaller. This corresponds to a unit cell volume that is too small by 3.8%. The difference between the static structure parameters from the model and the crystallographic values for structures with thermal averaging is roughly consistent with the size of the vibrational

TABLE 5: Structural Parameters and Energies of Large, Symmetric Acetylene Clusters

cluster symmetry cubic	structural parameters			MMC interaction energy (cm^{-1})
	$a = b = c$ (Å)	θ_1 (degrees)[a]	θ_2 (degrees)	
79	6.034	35.3	45.0	−115 805
201	6.023	35.3	45.0	−330 871
391	6.015	35.3	45.0	−684 601
expt.[b] [ref 37]	6.094	35.0	45.0	

cluster symmetry orthorhombic	structural parameters				MMC interaction energy (cm^{-1})
	a (Å)	b (Å)	c (Å)	θ_1 (degrees)	
79	6.502	6.462	5.628	50.3	−97 598
201	6.510	6.454	5.601	50.4	−276 208
391	6.510	6.450	5.586	50.4	−578 969
expt.[c] [ref 37]	6.198	6.023	5.578	50.3	

[a] Each molecule is twisted out of the $a-b$ plane by θ_1 and about the c-axis by θ_2. [b] Crystal structure of cubic acetylene (C_2H_2) measured at 131 K and a vapor pressure of 7.3 KPa. [c] Crystal structure of orthorhombic deuterioacetylene (C_2D_2) measured at 15 K and a vapor pressure of 7.3 KPa.

effect seen for rotational constants of the smaller clusters (Table 2). For the *c* unit cell parameter of the orthorhombic form, which is the distance between adjacent layers in the crystal, the agreement with the experimentally determined value is again about 1%. Also, the calculated orientations of the molecules in both solid forms are in very good agreement with experiment. However, the *a* and *b* unit cell parameters are larger than the experimental values by 4.8% and 6.6% in the orthorhombic crystal, and this corresponds to a unit cell volume 13% larger than experiment.

The orthorhombic crystal appears to have a special anisotropy in its potential such that the potential for compressing orthorhombic clusters along the *a* and *b* directions can be characterized as soft. For instance, we find only an 8 cm^{-1} per T-pairing energy change (out of ∼360) in the orthorhombic 79-membered cluster upon reducing the *a* and *b* unit cell parameters a substantial amount, 0.20 Å and 0.26 Å, respectively. This corresponds to reducing the difference between the calculated parameters for the 79-membered cluster (Table 5) and the crystallographic value by 2/3, selecting that reduction because we do not expect the finite cluster to fully display the structure of the infinite array of acetylenes. The compressiveness revealed by this calculation is for an accordion-like squeezing of the planar herringbone pattern of the acetylenes in the orthorhombic crystal.

In contrast to the herringbone planes of the orthorhombic crystal, the cubic crystal exhibits 3-dimensional interlocking with more molecule−molecule T-shaped connections. Consequently, the potential elements important in describing the two forms differ somewhat. In particular, the herringbone pattern can maintain the strength of the quadrupole−quadrupole interactions over a sizable distance range. It is therefore less sensitive to this potential element than the cubic form. In turn, this means that accurate description of the orthorhombic crystal calls for high accuracy for the close-in or contact pieces of the potential. With the use of simple 6−12 potentials in MMC, the close-in potential is represented very simply, and the error in the *a* and *b* unit cell parameters from MMC (Table 5) could easily be due to needing something better for the close-in repulsive part of the potential.

To analyze the energy difference between the cubic and orthorhombic forms, we carried out a 2-parameter fit of the MMC cluster energies for the 201- and 391-membered clusters of both types. On the basis of how these clusters were constructed, we took the 201 cluster as having 79 interior molecules and 122 exterior, and the 391 cluster as having 201 interior and 190 exterior. We then did a fit of the energies to a function which is linear in the number of interior molecules and in the number of exterior molecules. For the energy per interior molecule, this yielded 1909 cm^{-1} for the orthorhombic form and 2172 cm^{-1} for the cubic form. These values divided by the number of pairings per molecule (4 and 6) become 477 and 362 cm^{-1}, respectively. The latter of these is very close to the 360 cm^{-1} energy per T-pairing estimated earlier from smaller cluster values, and this goes along with our observation that the optimized smaller clusters most resemble the cubic crystal. The energy per pairing in the orthorhombic form by this analysis is very nearly the energy of the dimer, and this is clearly the result of the better-but-fewer tradeoff in the orthorhombic form.

The energy difference for the static structure of the 391-membered cluster places the cubic form below (more stable) than the orthorhombic form even though it is known to be the high-temperature form. This ordering also results if we apply the 362 and 477 cm^{-1} per T-pairing values to infinite clusters, giving 26.0 kJ mol^{-1} for the cubic lattice energy and 22.8 kJ mol^{-1} for the orthorhombic crystal. Of course, there are also vibrational zero-point energies contributions to the lattice energies, and these may be relatively important in view of the closeness of these two values. There is a body of infrared and Raman spectra for solid acetylene[40−44,64−69] that gives information on the intramolecular vibrational frequencies. It is clear that the stretching modes have lower frequecnies in the crystal than in the gas phase, while the bending modes have higher frquencies. These are opposed effects and while the sizes of these effects are different for the two crystal forms, the net effect is small in both, less than 0.2 kJ mol^{-1}. The zero-point contribution of the weak or intermolecular vibrations is more significant and we have tried to evaluate that within a harmonic picture and the MMC model potential.

We carried out an MMC calculation for the vibrational frequencies of the central acetylene embedded in 79-, 201-, and 391-membered clusters. The values are in Table 6. The closeness of the 201- and 391-cluster results shows that there is little effect of the cluster surface on the central molecule's vibrational potential with a cluster size of 201. The frequencies obtained by this type of calculation do not correspond directly to lattice vibrational frequencies mostly because of the neglect of coupling between molecules and the fact that they are harmonic. Regardless of what mixing would occur in an analysis of the true vibrations, the zero-point energy would not be changed sharply if the analysis were harmonic and if there was no translational−librational mixing.[70] Hence, we expect these values to serve as a workable estimate for determining the crystal energies. Combining values based on the 391-membered cluster with the static-structure energies yields a lattice energy of 21.9 kJ mol^{-1} for the cubic form and 19.2 kJ mol^{-1} for the

TABLE 6: Harmonic Intermolecular Vibrational Frequencies of an Acetylene Monomer in Crystal Fragments[a]

	cubic crystal fragments			orthorhombic crystal fragments		
cluster size	79	201	391	79	201	391
vibrational frequencies (cm^{-1})						
transl.	92	94	94	73	75	75
transl.	92	94	94	93	95	96
transl.	114	116	117	105	106	106
libration	190	192	192	138	140	140
ibration	190	192	192	188	188	189
ZPE	340	344	345	299	302	303

[a] The frequencies are calculated as the harmonic frequencies of the central acetylene with the remainder of crystal treated as rigid.

orthorhombic form from the MMC potential. The measured value for the low-temperature form is 21.5 kJ mol^{-1}.[71] Thus, our model potential provides a reasonable determination of the crystal lattice energy, and it places the two crystal forms very close in energy, though in the reverse order. This problem we associate with the accuracy needed for the critical balance of potential elements in the herringbone arrangement of the orthorhombic form. There may also be small contributions from other effects. For instance, we carried out a calculation that included 3-body dipole−dipole−dipole dispersion[72] and found that the energy contribution is more destabilizing for the cubic form than the orthorhombic form; that is, this element in a potential would provide a step toward the right energetic ordering. However, it is at most a small contribution given that scaling our guess value for the coefficient in this 3-body term a bit beyond a reasonable size compared to other species[73] could lead to at most 0.5 kJ mol^{-1} difference between the crystal forms. It is likely that that the two crystal forms are very close in their lattice energies and that the correct ordering comes about with a collection of small refinements, including other many-body effects.[74] As well, this points to the prospect of offsetting error sources, rather than arriving at a true potential, when the reworking of elements in a simple potential is done only so as to match orthorhombic values.

Summary

We have used a model potential based on the MMC representation of intermolecular interaction and extensive ab initio calculations on the acetylene dimer to study clusters of 3- to 391-acetylenes. Acetylene molecules have the capability to arrange with many near T-shaped pairings that offer stability through quadrupole−quadrupole interactions. As a result, the optimum form of the pentamer is found to be "4 + 1" with 8 near T-shaped pairings. The hexamer is "1 + 4 + 1" with S_4 symmetry, which is a four-membered ring with monomers above and below. Small distortions can interchange the S_4 axis with either of the other two axes, and there is a minimum energy structure only slightly different in energy from the global minimum in which the above and below acetylenes are parallel. Hence, there are a number of interesting, complicated, low-energy interconversion paths available to this system.

As cluster size increases to 13, the optimum structure resembles fragments of the cubic crystal. The cubic arrangement offers more T-shaped pairings than does an orthorhombic structure. However, the energy per pairing for an orthorhombic arrangement is better (477 vs 362 cm^{-1}), and hence, the two crystal forms can exist at energies that are very close. A number of small potential elements may be crucial to a critical determination of the difference in the lattice energy of the two forms.

Through our model calculations, we have sought to provide a picture of aggregation from the dimer to crystal fragments. The model, though simple, provides good-quality determinations of rotational constants of clusters, accurate values of most structural parameters of the crystal forms, and a lattice energy that agrees to 10% with measurement.[71] The connection in describing few through many acetylenes highlights the physical basis for the specific elements used in the model potential—that these are largely genuine to the interaction.

Acknowledgment. This work was supported, in part, by a grant from the Physical Chemistry Program of the National Science Foundation (CHE-9714016).

References and Notes

(1) Miller, R. E.; Vohralik, P. F.; Watts, R. O. *J. Chem. Phys.* **1984**, *80*, 5453.
(2) Prichard, D. G.; Nandi, R. N.; Muenter, J. S. *J. Chem. Phys.* **1988**, *89*, 115.
(3) Fraser, G. T.; Suenram, R. D.; Lovas, F. J.; Pine, A. S.; Hougen, J. T.; Lafferty, W. J.; Muenter, J. S. *J. Chem. Phys.* **1988**, *89*, 6028.
(4) Ohshima, Y.; Matsumoto, Y.; Takami, M.; Kuchitsu, K. *Chem. Phys. Lett.* **1988**, *147*, 1.
(5) Bryant, G. W.; Eggers, D. F.; Watts, R. O. *J. Chem. Soc., Faraday Trans. 2* **1988**, *84*, 1443.
(6) Colussi, A. J.; Sander, S. P.; Friedl, R. R. *Chem. Phys. Lett.* **1991**, *178*, 497.
(7) Matsumura, K.; Lovas, F. J.; Suenram, R. D. *J. Mol. Spectrosc.* **1991**, *150*, 576.
(8) Bhattacharjee, R. L.; Muenter, J. S.; Coudert, L. H. *J. Chem. Phys.* **1992**, *97*, 8850.
(9) Booze, J. A.; Baer, T. *J. Chem. Phys.* **1993**, *98*, 186.
(10) Zhu, Y. F.; Allman, S. L.; Phillips, R. C.; Garret, W. R.; Chen, C. H. *Chem. Phys. Lett.* **1994**, *224*, 7.
(11) Buck, U.; Ettischer, I.; Schulz, S. *Zeit. Phys. Chemie* **1995**, *188*, 91.
(12) Aoyama, T.; Matsuoka, O.; Nakagawa, N. *Chem. Phys. Lett.* **1979**, *67*, 508.
(13) Alberts, I. L.; Rowlands, T. W.; Handy, N. C. *J. Chem. Phys.* **1988**, *88*, 3811.
(14) Petrusova, H.; Havlas, Z.; Hobza, P.; Zahradnik, R. *Collect. Czech. Commun.* **1988**, *53*, 2495.
(15) Bone, R. G. A.; Handy, N. C. *Theor. Chim. Acta* **1990**, *78*, 133.
(16) Hobza, P.; Selzle, H. L.; Schlag, E. W. *Collect. Czech. Commun.* **1992**, *57*, 1186.
(17) Karpfen, A. *J. Phys. Chem. A* **1999**, *103*, 11431.
(18) Resende, S. M.; De Almeida, W. B. *Chem. Phys.* **1996**, *206*, 1.
(19) Shuler, K.; Dykstra, C. E. *J. Phys. Chem. A* **2000**, *104*, 4562.
(20) Bryant, G. W.; Eggers, D. F.; Watts, R. O. *Chem. Phys. Lett.* **1988**, *151*, 309.
(21) Prichard, D.; Muenter, J. S. *Chem. Phys. Lett.* **1987**, *135*, 9.
(22) Yu, J.; Su, S.; Bloor, J. E. *J. Phys. Chem.* **1990**, *94*, 5589.
(23) Bone, R. G. A.; Amos, R. D.; Handy, N. C. *J. Chem. Soc., Faraday Trans.* **1990**, *86*, 1931.
(24) De Almeida, W. B.; Hinchliffe, A. *J. Mol. Structure (THEOCHEM)* **1991**, *228*, 191.
(25) Brenner, V.; Millie, Ph. *Z. Phys. D* **1994**, *30*, 327.
(26) Bone, R. G. A.; Murray, C. W.; Amos, R. D. *Chem. Phys. Lett.* **1989**, *161*, 166.
(27) Bone, R. G. A.; Rowlands, T. W.; Handy, N. C.; Stone, A. J. *Mol. Phys.* **1991**, *72*, 33.
(28) De Almeida, W. B.; Hinchliffe, A.; Craw, J. S. *J. Mol. Struct. (THEOCHEM)* **1990**, *208*, 15.
(29) Dykstra, C. E. *J. Am. Chem. Soc.* **1990**, *112*, 7540.

(30) Sugawara, T.; Kanda, E. *Science Rept. Res. Inst., Tohoku University Ser. A* **1952**, *4*, 607.
(31) Koski, H. K.; Sandor, E. *Acta Crystallogr. B* **1975**, *31*, 350.
(32) Koski, H. K. *Acta Crystallogr. B* **1975**, *31*, 933.
(33) Koski, H. K. *Cryst. Struct. Commun.* **1975**, *4*, 343.
(34) Koski, H. K. *Cryst. Struct. Commun.* **1975**, *4*, 337.
(35) Koski, H. K. *Z. Naturforsch.* **1975**, *30a*, 1028.
(36) van Nes, G. J. H.; van Bolhuis, F. *Acta Crystallogr. B* **1979**, *35*, 2580.
(37) McMullan, R. K.; Kvick, A.; Popelier, P. *Acta Crystallogr. B* **1992**, *48*, 726.
(38) LeSar, R. *J. Chem. Phys.* **1987**, *86*, 1485.
(39) Bernasconi, M.; Chiarotti, G. L.; Focher, P.; Parrinello, M.; Tosatti, E. *Phys. Rev. Lett.* **1997**, *78*, 2008.
(40) Aoki, K.; Usuba, S.; Yoshida, M.; Kakudate, Y.; Tanaka, K.; Fujiwara, S. *J. Chem. Phys.* **1988**, *89*, 529.
(41) Aoki, K.; Kakudate, Y.; Usuba, S.; Yoshida, M.; Tanaka, K.; Fujiwara, S. *J. Chem. Phys.* **1988**, *88*, 4565.
(42) Aoki, K.; Kakudate, Y.; Yoshida, M.; Usuba, S.; Tanaka, K.; Fujiwara, S. *Solid State Commun.* **1987**, *64*, 1329.
(43) Aoki, K.; Kakudate, Y.; Yoshida, M.; Usuba, S.; Tanaka, K.; Fujiwara, S. *Synt. Met.* **1989**, *28*, D91.
(44) Sakashita, M.; Yamawaki, H.; Aoki, K. *J. Phys. Chem.* **1996**, *100*, 9943.
(45) Hirshfeld, F. L.; Mirsky, K. *Acta Crystallogr.* **1979**, *A35*, 366.
(46) Filippini, G.; Gramaccioli, C. M.; Simonetta, M. *J. Chem. Phys.* **1980**, *73*, 1376.
(47) Gamba, Z.; Bonadeo, H. *J. Chem. Phys.* **1982**, *76*, 6215.
(48) Gamba, Z.; Bonadeo, H. *J. Chem. Phys.* **1984**, *81*, 4724.
(49) Marchi, M.; Righini, R. *Chem. Phys.* **1985**, *94*, 465.
(50) Nyburg, S. C.; Faerman, C. H. *Mol. Phys.* **1989**, *67*, 447.
(51) Grabowski, S. J. *J. Chem. Res. (S)* **1996**, 534.
(52) Klein, M. L.; McDonald, I. R. *Chem. Phys. Lett.* **1981**, *80*, 76.
(53) Binbrek, O. S.; Anderson, A. *Phys. Stat. Sol. B* **1992**, *173*, 561.
(54) Leech, J. W.; Grout, P. J. *J. Phys.: Condens. Matter* **1993**, *5*, 1299.
(55) Santikary, P.; Bartell, L. S. *J. Phys. Chem.* A **1997**, *101*, 1299.
(56) Dykstra, C. E. *J. Am. Chem. Soc.* **1989**, *111*, 6168.
(57) Dykstra, C. E.; Liu, S.-Y.; Malik, D. J. *Adv. Chem. Phys.* **1989**, *75*, 37.
(58) Anderson, J. B. *J. Chem. Phys.* **1975**, *63*, 1499.
(59) Buch, V. *J. Chem. Phys.* **1992**, *97*, 726.
(60) Franken, K. A.; Dykstra, C. E. *J. Chem. Phys.* **1994**, *100*, 2865; *Chem. Phys. Lett.* **1994**, *200*, 161.
(61) Gregory, J. K.; Clary, D. C. *Chem. Phys. Lett.* **1994**, *228*, 547.
(62) Quack, M.; Suhm, M. A. *J. Chem. Phys.* **1991**, *95*, 28.
(63) Hollenstein, H.; Marquardt, R. R.; Quack, M.; Suhm, M. A. *J. Chem. Phys.* **1994**, *101*, 3588.
(64) Bottger, G. L.; Eggers, D. F. *J. Chem. Phys.* **1964**, *40*, 2010.
(65) Anderson, A.; Smith, W. H. *J. Chem. Phys.* **1966**, *44*, 4216.
(66) Schwartz, Y. A.; Ron, A.; Kimel, S. *J. Chem. Phys.* **1969**, *51*, 1666.
(67) Ito, M.; Yokoyama, T.; Suzuki, M. *Spectrochim. Acta* **1970**, *26A*, 695.
(68) Schwartz, Y. A.; Ron, A.; Kimel, S. *J. Chem. Phys.* **1971**, *54*, 99.
(69) Anderson, A.; Andrews, B.; Torrie, B. H. *J. Raman Spectrosc.* **1985**, *16*, 202.
(70) In separate harmonic analysis of translational (librational) weak modes, the masses (moments of inertia) would be identical for all molecules, and thus, any potential coupling ignored in our single-molecule analysis could give rise to a unitary transformation of normal coordinates. The mixing of vibrations that goes along with a unitary transformation would leave the trace of the force matrix unchanged. Hence, the sum of the squares of the vibrational frequencies would be unchanged. To the extent that the frequencies are similar in size—all are within a 100 cm^{-1} range—the invariance of the sum of the squares of the frequencies implies little change in the sum of the frequencies.
(71) McIntosh, D. *J. Phys. Chem.* **1907**, *11*, 306.
(72) Axilrod, B. M.; Teller, E. *J. Chem. Phys.* **1943**, *11*, 299.
(73) Kumar, A.; Meath, W. J. *Mol. Phys.* **1985**, *54*, 823.
(74) Meath, W. J.; Aziz, R. A. *Mol. Phys.* **1984**, *52*, 225.